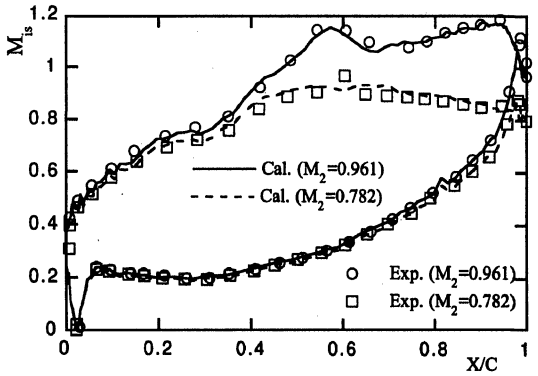

Fig. 3 Isentropic surface Mach number distributions for different values of M_2.

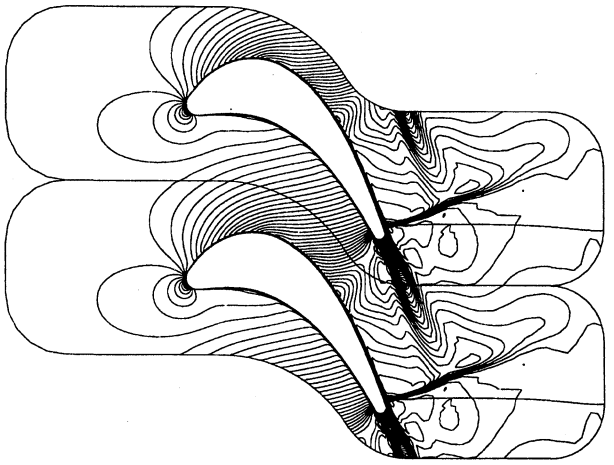

Fig. 4 Mach number contours for the VKI turbine cascade flow, M_2 = 0.961.

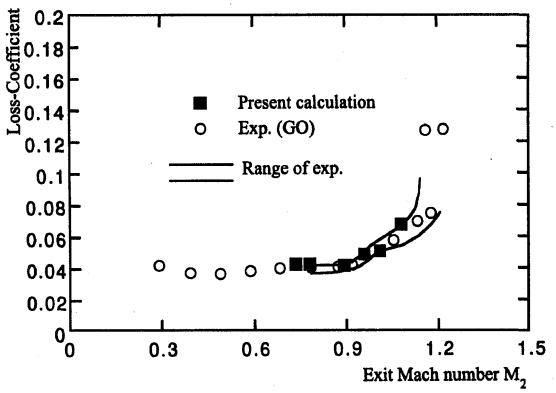

Fig. 5 Variation of loss coefficient with exit Mach number.

Figure 4 shows a clean capturing of the shock for transonic flow calculation. Figure 5 presents a comparison between experimental and computed loss coefficients. Calculated results agree favorably with the experimental data in both behavior and absolute values.

Conclusion

Subsonic and transonic flows through the VKI turbine cascade are calculated adopting the k–ω turbulence model. An explicit fourth-order Runge–Kutta solver for the Navier–Stokes equations and an implicit approximate factorization scheme for the k–ω equations are proposed. This mixed explicit–implicit time-marching scheme has proven to be fast, stable, and accurate, requiring less computer capacity than conventional fully implicit time-stepping schemes.

Acknowledgments

The authors would like to express their gratitude to the Turbo and Power Machinery Research Center of Seoul National University and Samsung Aerospace Industries, Ltd., for their support extended through the course of the present study.

References

[1]Arnone, A., and Swanson, R. C., "A Navier–Stokes Solver for Turbomachinery Applications," *Journal of Turbomachinery*, Vol. 115, No. 2, 1993, pp. 305–313.

[2]Lakshminarayana, B., "An Assessment of Computational Fluid Dynamic Techniques in the Analysis and Design of Turbomachinery—The 1990 Freeman Scholar Lecture," *Journal of Fluids Engineering*, Vol. 113, No. 3, 1991, pp. 315–352.

[3]Patel, V. C., Rodi, W., and Scheuerer, G., "Turbulence Models for Near-Wall and Low Reynolds Number Flows: A Review," *AIAA Journal*, Vol. 23, No. 9, 1985, pp. 1308–1319.

[4]Wilcox, D. C., "Reassessment of the Scale-Determining Equation for Advanced Turbulence Models," *AIAA Journal*, Vol. 26, No. 11, 1988, pp. 1299–1310.

[5]Menter, F. R., "Performance of Popular Turbulence Models for Attached and Separated Adverse Pressure Gradient Flows," AIAA Paper 91-1784, June 1991.

[6]Turner, M. G., and Jennions, I. K., "An Investigation of Turbulence Modelling in Transonic Fans Including a Novel Implementation of an Implicit k–ε Turbulence Model," *Journal of Turbomachinery*, Vol. 115, No. 2, 1993, pp. 249–260.

[7]Patankar, S. V., *Numerical Heat Transfer and Fluid Flow*, Hemisphere, New York, 1980.

[8]Wilcox, D. C., "Progress in Hypersonic Turbulence Modelling," AIAA Paper 91-1785, 1991.

[9]Kiock, R., Lehthaus, F., Baines, N. C., and Sieverding, C. H., "The Transonic Flow Through a Plane Turbine Cascade as Measured in Four European Wind Tunnels," *Journal of Engineering for Gas Turbines and Power*, Vol. 108, No. 2, 1986, pp. 277–284.

S. Fleeter
Associate Editor

Numerical Simulations of Three-Dimensional Trailing Vortex Evolution

Robert E. Robins* and Donald P. Delisi†
NorthWest Research Associates, Inc.,
Bellevue, Washington 98009-3027

I. Introduction

IT is well known that trailing vortices in unstratified, unsheared fluid, out of ground effect, will undergo an instability that results in the periodic linking of the initially parallel vortex tubes and the formation of vortex rings. Evidence of this instability was first noted by Scorer.[1]

Crow[2] first explained this phenomenon (hence, it is now called Crow instability) by performing a perturbation analysis of the kinematic relation between velocity and vorticity and found that 1) the wavelength of maximum perturbation growth (which we denote as λ^*) is $8.6b_0$, where b_0 is the initial distance between the parallel vortices; 2) the perturbation amplitude grows by a factor of e ($\cong$ 2.72) in a time equivalent to $1.21T_0$, where T_0 is the time required for the vortices to descend a distance equal to b_0, i.e., $T_0 = b_0/V_0$, where V_0 is the initial descent speed, given by $\Gamma_0/2\pi b_0$, Γ_0 being the initial magnitude of the circulation about each of the vortices; 3) the angle to the horizontal of the plane in which the initial maximum growth occurs is 48 deg; and 4) λ^* increases as the size of the vortex cores decreases. Result 2 is characterized by

Received Nov. 7, 1995; revision received March 3, 1997; accepted for publication May 27, 1997.

*Research Scientist, P.O. Box 3027. Member AIAA.
†Senior Research Scientist, P.O. Box 3027. Member AIAA.

the equation $A/A_0 = \exp(t/1.21T_0)$, where A is perturbation amplitude, t is time, and A_0 is the initial value of A. Results 1–3 are derived by Crow, and result 4 may be inferred from Fig. 10 of Ref. 2. Result 4 is also apparent in Fig. 5 of Widnall's review.[3]

We note that Crow[2] used a specific vortex characterization in performing his analysis. Namely, he assumed uniform vorticity throughout the cores of the vortices and zero vorticity outside the cores. He based his choice of core diameter ($0.20b_0$) and the size of an interval required to avoid an integral singularity on the previously published results of Spreiter and Sacks[4] and Thomson.[5]

In this Note, we present results from simulations of Crow instability obtained by using a computer code to numerically solve the three-dimensional, nonlinear Navier–Stokes equations for an incompressible fluid. We show that these results agree with Crow's results, thus validating the code. In addition, by depicting the full nonlinear evolution of the instability, our results extend Crow's results to later times. This validation of the code lays the groundwork for using it in future studies on how Reynolds number, stratification, shear, and ground effect influence three-dimensional evolution of aircraft wake vortices.

To model the trailing vortices produced by an aircraft, we have chosen a numerical approach that focuses on a portion of the wake that is large enough to permit initially perturbed vortices to link and form rings but small enough to run on existing computers. Also, we assume that the vortex evolution occurs far enough behind the aircraft that axial velocities in the vortices can be ignored. Crow's study[2] provides important guidance in deciding how large the portion of the wake to be modeled should be. His key result is that the linking instability undergoes maximum growth for a perturbation wavelength of $8.6b_0$. Thus, a computational domain of about this length should be large enough to permit the formation of vortex rings.

II. Numerical Approach

The code we have used solves the primitive three-dimensional Navier–Stokes equations for an incompressible fluid. It uses a two-step projection method, based on the work of Chorin,[6] to evolve the solution in time while ensuring incompressibility. The first step advects the flow using a second-order Adams–Bashforth scheme and is followed by a projection step, which relies on a fast Poisson solver. The side wall boundary conditions are periodic, and fast Fourier transforms are used to compute horizontal derivatives. For simplicity, the boundary conditions at the top and bottom of the computational domain are rigid-lid/free-slip. A sixth-order compact scheme, similar to one described by Lele,[7] is used to compute vertical derivatives. The two-thirds rule, discussed by Canuto et al.,[8] is used to avoid aliasing. Fourier and compact low-pass filters, in the horizontal and vertical directions, respectively, are used to control the build-up of small-scale energy. The compact filter is also based on a scheme described by Lele.[7]

The calculations of trailing vortex evolution, discussed in the next section, are initialized by either a single pair of counter-rotating vortices (Sec. III.A) or a superposition of such pairs (Sec. III.B). The horizontal coordinate aligned with the axes of the vortices is denoted by x, the horizontal cross-axial coordinate by y, and the vertical coordinate by z. Initially, the axes of the vortices lie in the same horizontal plane and are slightly perturbed from being parallel straight lines. The perturbation is sinusoidal, with each sinusoid in the single wavelength cases having a peak-to-peak amplitude equal to 2% of b_0, the nominal distance between the vortices. The sinusoids are 180 deg out of phase; thus, the separation between the vortices varies from 1.02 to 0.98 times b_0. In planes perpendicular to the x coordinate, the vortices have either uniform or Gaussian circular vorticity distributions. The cores of the vortices are defined by r_0. For uniform vortices, this is the radius within which the vorticity is constant and outside of which the vorticity is zero. For Gaussian vortices, r_0 is the value at which the vorticity falls to $1/e$ of its peak value. The migration direction of the vortices is downward, to simulate vortices produced by aircraft. When the vortices approach within $2b_0$ of the lower boundary of the computational domain, the domain is shifted downward relative to the vortices, and the calculation is continued.

Numerical accuracy of all computational results was ensured by monitoring the quantity $\varepsilon = \text{SQRT}\ (\langle \text{DIV}^2 \rangle / \langle \text{GRADSQ} \rangle)$, where $\text{DIV} = \partial u/\partial x + \partial v/\partial y + \partial w/\partial z$, $\text{GRADSQ} = (\partial u/\partial x)^2 + (\partial v/\partial y)^2 + (\partial w/\partial z)^2$, and $\langle\ \rangle$ indicates an average over the computational domain; here, u, v, and w are the flow velocity components in the x, y, and z directions. The quantity ε is a measure of the incompressibility of computed flows; the value of ε for an incompressible flow should be zero. Our criterion for a calculation to be of acceptable accuracy was that the value of ε at the conclusion of the calculation be less than 0.01. This criterion was satisfied for all computed flows presented subsequently.

III. Results

A. Single-Wavelength Cases

We first describe a set of results for which each calculation was initialized using a single vortex pair having wave number one in the x direction. The number of grid points for each case was $NX \times NY \times NZ = 65 \times 129 \times 181$, where NX, NY, and NZ are the numbers of grid points in the x, y, and z directions. The spatial resolution was equal in the y and z directions, and 24 grid points separated the vortices in the y direction. In the x direction, the grid spacing depended on the perturbation wavelength (discussed subsequently). For all cases, the Reynolds number Re was 2930, where $Re = \Gamma_0/\nu$, with ν being the kinematic viscosity. The time step for all cases was $T_0/449$.

A total of 20 single wavelength cases was computed using two initial vorticity distribution types, two values of the core radius, and five perturbation wavelengths. We used both uniform and Gaussian vorticity distributions, and the radii were $0.10b_0$ (10% core) and $0.16b_0$ (16% core). The five wavelengths were chosen to be 6.6, 7.6, 8.6, 9.6, and 10.6 times b_0 (yielding axial spatial resolutions from $0.103b_0$ to $0.166b_0$). These cases include the vortex model analyzed by Crow[2] (uniform vorticity core and a core radius of $0.10b_0$) and the wavelength ($8.6b_0$) predicted by Crow to have the most rapid perturbation growth.

For each case, we determined the perturbation amplitude as a function of time. Figure 1a shows results at $2T_0$, $3T_0$, and $4T_0$, and Fig. 1b shows results at $4T_0$, $5T_0$, and $6T_0$. The vertical axes represent peak-to-peak perturbation amplitude, and the horizontal axes represent perturbation wavelength, both in terms of b_0. The curves are second-order, least square fits to the data points. Note that all perturbation amplitudes were measured in the plane of maximum perturbation growth.

Figure 1 shows that the amplitudes are greater for the $0.10b_0$ core cases than for the $0.16b_0$ core cases. This implies that trailing vortices with tight cores will link and form rings more quickly than those with broad cores. It is also evident from the results at $2T_0$ and $3T_0$ that the behaviors for the uniform and Gaussian core cases are quite similar. We thus omit the uniform core results for $4T_0$ because they again are nearly the same as the Gaussian core results. We note that this similarity is probably due to the inability of the numerical solution to adequately resolve and maintain the sharp transition (from zero vorticity to constant vorticity) that is characteristic of the uniform vorticity model. Thus, Gaussian vorticity cores are likely to be a more suitable choice than uniform cores for computing trailing vortex evolution with our numerical model.

From Fig. 1a, it is difficult to determine a wavelength of maximum perturbation growth from the results at $2T_0$. By a time of $3T_0$, however, it is clear that $\lambda^* \sim 9b_0$ and $\lambda^* \sim 8.5b_0$ are the approximate maximum growth wavelengths for the 10% core case and the 16% core case, respectively. These results are in good agreement with Crow's prediction of $\lambda^* = 8.6b_0$ (for vortices with 10% uniform cores). These results also agree with the inference from Crow[2] that vortices with smaller cores should have larger values of λ^* (result 4 in the Introduction).

For times greater than $3T_0$, the perturbation growth accelerates dramatically. Consequently, results for $4T_0$, $5T_0$, and $6T_0$ are plotted on an expanded vertical scale in Fig. 1b. Only results for the Gaussian core cases are shown because they are nearly identical to results for the uniform core cases.

By the times of $5T_0$ and $6T_0$ for the 10% core case and the 16% core case, respectively, the perturbation amplitude shows a distinct

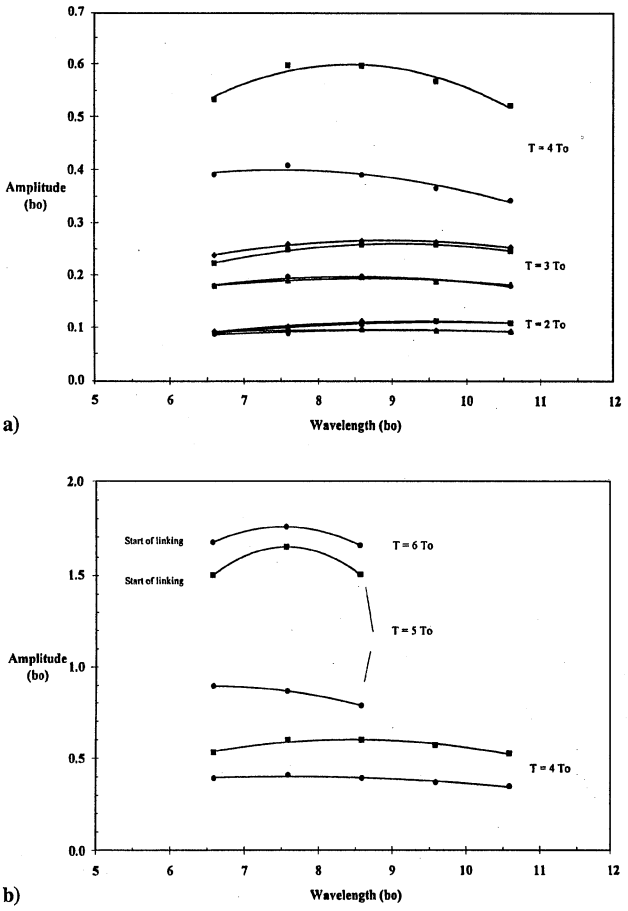

Fig. 1 Peak-to-peak perturbation amplitude vs wavelength for the single-wavelength case: ♦, 10% uniform core; ■, 10% Gaussian core; ▲, 16% uniform core; and ●, 16% Gaussian core; solid lines are second-order, least square fits to the data points at the indicated times.

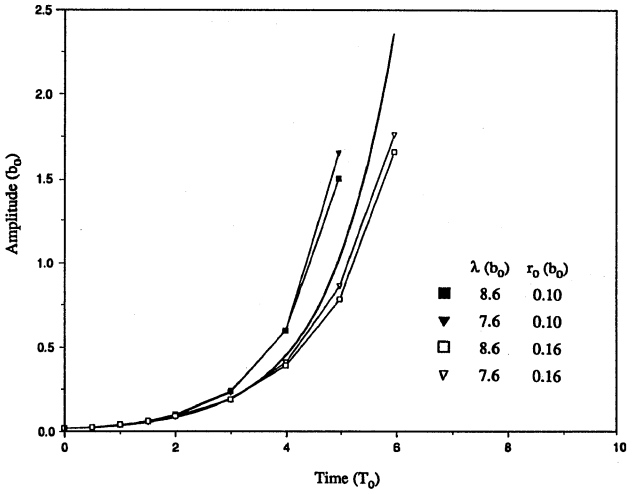

Fig. 2 Computed peak-to-peak amplitude vs time for four single-wavelength cases identified by symbols along with the growth predicted by Crow (——) (all vortices have an initially Gaussian vorticity distribution); ■, cases closest to that analyzed by Crow.[2]

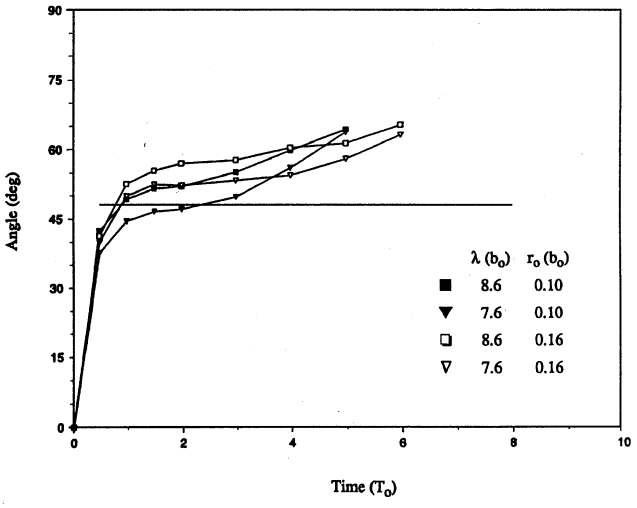

Fig. 3 Computed angle vs time for the four single-wavelength cases in Fig. 2 (symbols) with Crow's prediction (——).

peak for a wavelength of $7.6b_0$. (Data points for wavelengths $9.6b_0$ and $10.6b_0$ at times $5T_0$ and $6T_0$ are omitted from Fig. 1b because they were not necessary to define the peaks at those times.) From examination of vortex magnitude surface plots, it is clear for each case that these times coincide with the onset of linking. Thus, although our numerical results show the largest initial growth for wavelength near the $8.6b_0$ predicted by Crow,[2] the most rapid growth at later times appears to take place at shorter wavelengths.

To compare our results to Crow's results, we analyzed the results from four selected runs at early times. The wavelengths for these runs were $7.6b_0$ and $8.6b_0$, and the vortex cores were 10 and 16% Gaussian. Figure 2 shows plots of the computed amplitude growth vs time for these four cases along with the growth predicted by Crow[2] (starting at $t = 0.5T_0$). We use the starting time of $0.5T_0$ for Crow's result because, as can be seen from Fig. 3, that is the time by which the initially horizontal perturbation planes of our computed results have become close enough to the 48 deg predicted by Crow for the comparisons to be meaningful. In Fig. 2, note the excellent agreement between the computed results and Crow's result for times $<\sim 2T_0$ and the approximate agreement between the computed result and Crow's perturbation results for later times.

Figure 3 shows the angle to the horizontal of the computed maximum growth planes vs time for the cases in Fig. 2. It is notable that, in all cases, the angle increases rapidly from 0 deg to an angle approximately equal to the 48 deg predicted by Crow and that this angle increases in later stages in the evolution.

We note several points from the results of the single-wavelength calculations presented in Figs. 1–3. First, the numerical model shows good agreement with Crow's[2] analysis described in the Introduction; that is, the numerical model shows good agreement at early times with Crow's predictions of the wavelength of maximum perturbation growth, the rate of growth of the perturbation amplitude, the angle to the horizontal of the plane of maximum growth, and the variation of the wavelength of maximum perturbation growth as a function of core size. We view this good agreement with Crow's results as a validation of the numerical model. Second, at later times ($t \sim 3T_0$–$4T_0$), the numerical model predicts a shift toward smaller wavelengths ($\sim 7.6b_0$) and larger angles (~55–60 deg) for the maximum growth. Third, although our initial perturbations are in a horizontal plane, the plane of maximum growth quickly evolves to around 48 deg, as predicted by Crow. Thus, the results presented here appear to be robust and at least relatively insensitive to the method of how the initial perturbation is prescribed. Fourth, the model predicts that smaller core vortices have faster growing perturbations (cf. Fig. 1b) and grow in planes at smaller angles to the horizontal than broader core vortices at early times (cf. Fig. 3). Finally, at times near linking, both the 10 and 16% core vortices are inclined at an angle of ~65 deg to the horizontal (cf. Fig. 3). Thus, the angle of the plane of maximum perturbations increases significantly from the initial value of near 48 deg to around 65 deg at linking.

B. Multiple-Wavelength Case

In the preceding subsection, the initial perturbations consisted of a single wavelength. However, real trailing vortices behind aircraft are perturbed by a spectrum of wavelengths. To model this more realistic case, we initialized our code with a trailing vortex composed of a superposition of 13 component trailing vortices, each having a

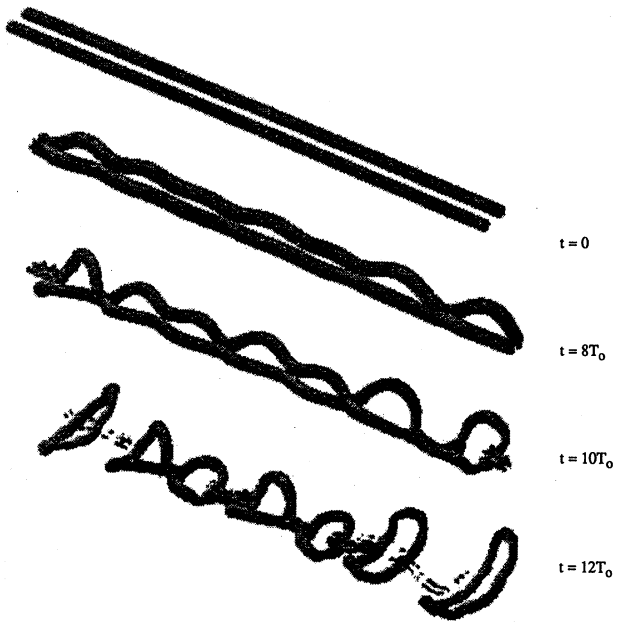

Fig. 4 Vorticity magnitude surfaces for trailing vortices evolving from an initial state perturbed by a spectrum of wavelengths; vertical distance between plots at different times is for illustration only and does not represent the distance traveled by the vortex system.

different perturbation wavelength. For reasons of computational efficiency, Gaussian 16% cores were used for each component vortex pair, and the resolution in the y, z plane was chosen to be half the resolution of the single-wavelength cases. The number of grid points in the computational domain was $NX \times NY \times NZ = 257 \times 65 \times 91$, and the length in the x direction, along the axes of the vortices, was $45.5b_0$. This length was chosen so that one of the component vortices would have a wavelength near $7.6b_0$ because this was the maximum growth wavelength at later evolution times, as seen from the single-wavelength results (cf. Fig. 1b).

The 13 component vortices ranged in wave number m from 4 to 16, which gave wavelengths equal to $11.38b_0$, $9.10b_0$, $7.58b_0$, $6.50b_0$, $5.69b_0$, $5.06b_0$, $4.55b_0$, $4.14b_0$, $3.79b_0$, $3.50b_0$, $3.25b_0$, $3.03b_0$, and $2.84b_0$. Each component was a nearly parallel pair of counter-rotating vortices, with their axes slightly perturbed from parallel as in the single-wavelength cases. As in Sec. III.A, the vortex axes were sinusoidal and 180 deg out of phase, and the peak-to-peak amplitude of each sinusoid was $0.02b_0$. The energies of the various component vortex pairs were chosen to scale as $m^{-5/3}$, and their relative phases were randomly selected. The energies were normalized so that the total circulation for the composite trailing vortex was the same as for the single wavelength cases. The maximum peak-to-peak amplitude of the trailing vortices formed from the 13 components was $0.008b_0$. This value is smaller than the $0.02b_0$ amplitude of each component because of the random selection of their relative phases. The Reynolds number and time step for this case were the same as for the preceding cases.

Figure 4 shows surface contour plots of vorticity magnitude for the initial, composite trailing vortices and for the evolved vortices at times of $8T_0$, $10T_0$, and $12T_0$. At $12T_0$, we see seven rings in various stages of development, each of which is clearly discernible at the time $8T_0$. Note that the irregularity in the sizes of the various rings is due to the use of multiple wavelengths. A single-wave-number calculation would have produced rings of identical size.

To identify the wavelengths for which the perturbation grows fastest, we examined spectra of the vertical velocity in a horizontal plane. Our results showed that the early dominant scale is about $8.6b_0$, the maximum growth wavelength predicted by Crow, but that by $10T_0$ the dominant scale is around $7b_0$. This result is consistent with the single-wavelength results, which showed that as the instability develops the maximum perturbation growth occurs at a wavelength less than $8.6b_0$. In recent laboratory studies, we have visualized trailing vortices undergoing linking instability and found that they evolve into rings having axial scales on the order of $5b_0$–$7b_0$. Thus, qualitatively at least, these laboratory observations confirm the results of our numerical calculations.

Our ultimate goal is to study the effects of Reynolds number, stratification, shear, and ground effect on the three-dimensional evolution of trailing vortices. The current study demonstrates the validity of our numerical approach and thus lays the foundation for these additional studies. Recent results showing Reynolds number and stratification effects appear in Delisi et al.[9] and Robins and Delisi,[10] respectively.

IV. Concluding Remarks

We have computed solutions that depict the evolution of trailing vortices, from initially having their axes slightly perturbed from parallel, through the early stages of perturbation growth, to the occurrence of linking, followed by the formation and migration of rings. Our results agree with the findings of Crow,[2] listed in the Introduction, the most significant of which is that the wavelength of maximum perturbation growth for vortices undergoing linking instability is initially about $8.6b_0$.

In addition, our results extend Crow's analysis by showing that linking occurs sooner for vortices with tighter cores, the maximum growth wavelength decreases as the instability evolves, and the angle of growth of the maximum perturbation evolves from around the 48 deg predicted by Crow[2] to near 65 deg at the time of linking. Finally, results for vortices composed of a superposition of components having different wavelengths show good agreement with laboratory results.

Acknowledgments

We thank the Office of Naval Research and the Naval Sea Systems Command for partial support of this work under Contracts N00014-89-C-0030 and N00024-91-C-6312, respectively, and we thank NASA's Numerical Aerodynamics Simulation Program for its helpful staff and a generous allocation of computer time. We also wish to thank George Greene, Jim Riley, and Philippe Spalart for useful discussions and encouragement and Don Slinn for advice on numerical matters.

References

[1]Scorer, R. S., "Condensation Trails," *Weather*, Vol. 10, No. 9, 1955, p. 281.

[2]Crow, S. C., "Stability Theory for a Pair of Trailing Vortices," *AIAA Journal*, Vol. 8, No. 12, 1970, pp. 2172–2179.

[3]Widnall, S. E., "The Structure and Dynamics of Vortex Filaments," *Annual Review of Fluid Mechanics*, Vol. 7, 1975, pp. 141–165.

[4]Spreiter, J. R., and Sacks, A. H., "The Rolling up of the Trailing Vortex Sheet and Its Effect on the Downwash Behind Wings," *Journal of the Aeronautical Sciences*, Vol. 18, No. 1, 1951, pp. 21–32.

[5]Thomson, W., "Vibrations of a Columnar Vortex," *Mathematical and Physical Papers*, Vol. 4, Cambridge Univ. Press, Cambridge, England, UK, 1910, pp. 152–165.

[6]Chorin, A. J., "Numerical Solution of the Navier–Stokes Equations," *Mathematics of Computation*, Vol. 22, No. 104, 1968, pp. 742–762.

[7]Lele, S. K., "Compact Finite Difference Schemes with Spectral-Like Resolution," *Journal of Computational Physics*, Vol. 103, Jan. 1992, pp. 16–42.

[8]Canuto, C., Hussaini, M. Y., Quarteroni, A., and Zang, T. A., *Spectral Methods in Fluid Dynamics*, Springer–Verlag, New York, 1988, pp. 84, 85.

[9]Delisi, D. P., Greene, G. C., Robins, R. E., and Singh, R., "Recent Laboratory and Numerical Trailing Vortex Studies," *Characterization and Modification of Wakes from Lifting Vehicles in Fluids*, AGARD-CP-584, Canada Communications Group, Hull/Quebec, PQ, Canada, 1996, pp. 264–270.

[10]Robins, R. E., and Delisi, D. P., "3-D Calculations Showing the Effects of Stratification on the Evolution of Trailing Vortices," *Computation of Three-Dimensional Complex Flows*, edited by M. Deville, S. Gavarlakis, and I. L..Rhyming, Notes on Numerical Fluid Mechanics, Vol. 53, Vieweg, Braunschweig, Germany, 1996, pp. 34-1–34-10.

A. Plotkin
Associate Editor